JP Journal of Heat and Mass Transfer

Published Online: February 2014
Available online at http://pphmj.com/journals/jphmt.htm
Volume 8, Number 2, 2013, Pages 187-210

FREE CONVECTIVE HEAT AND MASS TRANSFER FLOW PAST AN OSCILLATING PLATE WITH HEAT GENERATION, THERMAL RADIATION AND THERMO-DIFFUSION EFFECTS

Sanjib Sengupta and Mausumi Sen

Department of Mathematics
Assam University
Silchar, Assam, India
e-mail: sanjib_aus2009@rediffmail.com

Department of Mathematics
NIT Silchar
Silchar, Assam, India
e-mail: sen_mausumi@rediffmail.com

Abstract

An exact analysis of the physical effects of thermo-diffusion (Soret) and thermal radiation on free convective unsteady two-dimensional heat and mass transfer flow of a thermally generating Newtonian viscous incompressible fluid on an oscillating vertical permeable surface is presented. The governing system of partial differential equations is transformed into a set of ordinary differential equations by using a set of periodic transformations. Cogly-Vincentine-Gilles equilibrium heat flux model is incorporated in the energy equation. Exact closed form of solutions for velocity, temperature and

Received: November 7, 2013; Accepted: January 28, 2014
Keywords and phrases: free convection, mass transfer, heat generation, thermal radiation, thermo diffusion.

concentration fields as well as skin-friction, Nusselt and Sherwood numbers are obtained in terms of various pertinent parameters present and are finally interpreted numerically through graphs and tables.

Nomenclature

$\overline{C}$	Species concentration
c_p	Specific heat at constant pressure
$\overline{C}_w$	Species concentration at the plate
$\overline{C}_\infty$	Species concentration in the free stream
D_M	Coefficient of mass diffusion
D_T	Coefficient of thermal diffusion
Gm	Thermal Grashof number
Gr	Solutal Grashof number
k	Thermal conductivity
Nu_R	Nusselt number (Real part)
Pr	Prandtl number
R	Radiation parameter
S	First-order heat source parameter
Sc	Schmidt number
Sh_R	Sherwood number (real part)
Sr	Soret number
t	Time variable (non-dimensional)
$\bar{t}$	Time variable (dimensional)
$\overline{T}$	Fluid temperature

$\overline{T}_w$ Temperature at the plate

$\overline{T}_\infty$ Temperature in the free stream

u First component of fluid velocity (non-dimensional)

$\overline{u}$ First component of fluid velocity (dimensional)

u_0 Mean plate velocity (non-dimensional)

U_0 Mean plate velocity (dimensional)

u_R Real part of u

y y-co-ordinate (dimensional)

$\overline{y}$ y-co-ordinate (non-dimensional)

v Second component of fluid velocity (non-dimensional)

V_0 Mean suction velocity

$\overline{v}$ Second component of fluid velocity (dimensional)

Greek Symbols

β Thermal coefficient of volumetric expansion

β^* Solutal coefficient of volumetric expansion

ρ Fluid density

ν Kinematic coefficient of viscosity

θ Non-dimensional temperature

ϕ Non-dimensional species concentration

θ_R Real part of θ

ϕ_R Real part of ϕ

τ_R Non-dimensional skin friction (real part)

ω Frequency of oscillation

Subscripts

w	Conditions on the walls
∞	Free stream conditions

1. Introduction

Unsteady oscillatory free convective flow with heat and mass transfer has been a subject of interest for many researchers because of its diverse applications in science and technology, which involve the interface of several phenomena. A simple unsteady flow, which sets up from rest when a plane surface oscillates with a prescribed periodic velocity, was first investigated by Stokes [22] and later by Rayleigh [18] and is thus called *Stoke's second problem* or *Rayleigh's problem*. After the pioneering works of Stoke's and Rayleigh, several other workers had contributed in unsteady flow problems like, Soundalgekar [21], Das [7], Gulab and Mishra [12], Megahed [16], Jain and Gupta [15] etc. Natural convection induced by the simultaneous action of buoyancy forces resulting from thermal and mass diffusion is of considerable interest in nature and in many industrial applications such as geophysics, oceanography, drying processes, solidification of binary alloy and chemical engineering. Researchers like Devi and Nagaraj [8], Gokhale and Samman [11] etc. are some of the notable contributors in unsteady heat and mass transfer phenomena. When heat and mass transfer occur simultaneously in a moving fluid, the relations between the fluxes and the driving potentials are of more intricate in nature. It has been observed that mass fluxes can also be created by temperature gradients, known as the thermal-diffusion or Soret effect, which has been utilized for isotope separation and in mixtures between gases with very light molecular weight like (H_2, He). The notable contribution in Soret effect was made by Eckert and Drake [10]. Hurle and Jakeman [14] considered the case of Soret-driven thermo-solutal convection. Significant work on Soret effect was also done by researchers like Dursunkaya and Worek [9], Postelnicu [17], Ahmed and Sengupta [1], Sengupta [19] etc. Of late Ahmed et al. [2] investigated Soret effect and obtained closed form of solution for MHD heat and mass transfer flow past

an oscillating plate. In several physical problems that are associated with the fast growth of electronic technology, effective cooling of electronic equipment and cooling of nuclear reactors, there is a need of study of heat generation or absorption effects in moving fluids. Chamkha [5] studied the unsteady MHD convective heat and mass transfer flow past a moving semi-infinite vertical porous plate with heat absorption. On the other hand, the science of thermal radiation has become of increasing importance in aerospace research and design due to high temperatures associated with increased engine efficiencies. The pioneering work in the field of radiation was made by Cess [4]. Hossain and Takhar [13] investigated the effect of radiation on mixed convection flow along a vertical plate with uniform surface temperature. Radiation effect on MHD mixed convection flow about a permeable vertical plate was examined by Aydin and Kaya [3]. Sengupta [20] considered the thermal radiation effect on mixed convective mass transfer flow with thermal diffusion and heat absorption.

In the present work, we propose to study the physical effects of Soret, thermal radiation and heat generation on a laminar two-dimensional unsteady free convective heat and mass transfer flow of an incompressible viscous fluid past an exponentially oscillating permeable plate.

2. Mathematical Formulation of the Problem

A co-ordinate system $(\bar{x}, \bar{y})$ has been introduced, with its $\bar{x}$-axis along the length of the plate in the upward vertical direction and $\bar{y}$-axis perpendicular to the plate towards the fluid region. Using Boussinesq and boundary layer approximations, a two-dimensional fluid model has been developed in terms of a system of coupled partial differential equations, combined with two point semi-open initio-boundary conditions as:

Continuity equation

$$\frac{\partial \bar{v}}{\partial \bar{y}} = 0. \tag{1}$$

Momentum equation

$$\frac{\partial \bar{u}}{\partial \bar{t}} + \bar{v}\frac{\partial \bar{u}}{\partial \bar{y}} = \nu \frac{\partial^2 \bar{u}}{\partial \bar{y}^2} + g\beta(\bar{T} - \bar{T}_\infty) + g\beta^*(\bar{C} - \bar{C}_\infty). \tag{2}$$

Energy equation

$$\frac{\partial \bar{T}}{\partial \bar{t}} + \bar{v}\frac{\partial \bar{T}}{\partial \bar{y}} = \frac{k}{\rho c_p}\frac{\partial^2 \bar{T}}{\partial \bar{y}^2} - \frac{1}{\rho c_p}\frac{\partial \bar{q}_{r\bar{y}}}{\partial \bar{y}} + \frac{\bar{Q}}{\rho c_p}(\bar{T} - \bar{T}_\infty). \tag{3}$$

Species continuity equation

$$\frac{\partial \bar{C}}{\partial \bar{t}} + \bar{v}\frac{\partial \bar{C}}{\partial \bar{y}} = D_M \frac{\partial^2 \bar{C}}{\partial \bar{y}^2} + D_T \frac{\partial^2 \bar{T}}{\partial \bar{y}^2}. \tag{4}$$

The relevant initio-boundary conditions:

$$\left.\begin{aligned} &\bar{u} = 0,\ \bar{T} = \bar{T}_\infty,\ \bar{C} = \bar{C}_\infty, \text{ for every } \bar{y} \text{ and when } \bar{t} \le 0 \\ &\bar{u} = U_0 \exp(i\bar{\omega}\bar{t}),\ \bar{T} = \bar{T}_w,\ \bar{C} = \bar{C}_w, \text{ at } \bar{y} = 0, \text{ when } \bar{t} > 0 \\ &\bar{u} \to 0,\ \bar{T} \to \bar{T}_\infty,\ \bar{C} \to \bar{C}_\infty, \text{ for } \bar{y} \to \infty, \text{ when } \bar{t} > 0 \end{aligned}\right\}. \tag{5}$$

On assuming the medium is optically thin with relatively low density and following Cogly-Vincentine-Gilles [6] equilibrium model, the radiative heat flux is quantified as

$$\frac{\partial \bar{q}_{\bar{y}}}{\partial \bar{y}} = 4I^*(\bar{T} - \bar{T}_\infty), \tag{6}$$

where

$$I^* = \int_0^\infty (k_{\lambda^*})_w \left(\frac{\partial e_{b\lambda^*}}{\partial \bar{T}}\right)_w d\lambda^*,$$

where k_{λ^*} is the absorption coefficient, $e_{b\lambda^*}$ is Plank's constant, λ^* represents wavelength. On using (6), (3) gives

$$\frac{\partial \overline{T}}{\partial \overline{t}} + \overline{v}\frac{\partial \overline{T}}{\partial \overline{y}} = \frac{k}{\rho c_p}\frac{\partial^2 \overline{T}}{\partial \overline{y}^2} - 4I^*(\overline{T} - \overline{T}_\infty) + \frac{\overline{Q}}{\rho c_p}(\overline{T} - \overline{T}_\infty). \tag{7}$$

We introduce the following non-dimensional quantities as:

$$y = \frac{\overline{y}V_0}{\nu},\ t = \frac{\overline{t}V_0^2}{\nu},\ u = \frac{\overline{u}}{U_0},\ v = \frac{\overline{v}}{V_0},\ Gr = \frac{g\beta\nu(\overline{T}_w - \overline{T}_\infty)}{U_0V_0^2},$$

$$Gm = \frac{g\beta^*\nu(\overline{C}_w - \overline{C}_\infty)}{U_0V_0^2},\ \omega = \frac{\overline{\omega}\nu}{V_0^2},\ \theta = \frac{\overline{T} - \overline{T}_\infty}{\overline{T}_w - \overline{T}_\infty},\ S = \frac{\overline{Q}\nu}{\rho c_p V_0^2},$$

$$\phi = \frac{\overline{C} - \overline{C}_\infty}{\overline{C}_w - \overline{C}_\infty},\ Pr = \frac{\nu\rho c_p}{k},\ Sc = \frac{\nu}{D_M},$$

$$Sr = \frac{D_T(\overline{T}_{w^*} - \overline{T}_\infty)}{\nu(\overline{C}_{w^*} - \overline{C}_\infty)},\ R = \frac{4I^*\nu^2}{kV_0^2}.$$

The non-dimensional form of equations (1), (7) and (3) is

$$\frac{\partial u}{\partial t} - \frac{\partial u}{\partial y} = \frac{\partial^2 u}{\partial y^2} + Gr\theta + Gm\phi, \tag{8}$$

$$Pr\left(\frac{\partial \theta}{\partial t} - \frac{\partial \theta}{\partial y}\right) = \frac{\partial^2 \theta}{\partial y^2} + (S - R)Pr\theta, \tag{9}$$

$$Sc\left(\frac{\partial \phi}{\partial t} - \frac{\partial \phi}{\partial y}\right) = \frac{\partial^2 \phi}{\partial y^2} + SrSc\frac{\partial^2 \theta}{\partial y^2}. \tag{10}$$

The corresponding non-dimensional initio-boundary conditions are:

$$\left.\begin{array}{l} u = 0,\ \theta = 0,\ \phi = 0, \text{ for every } y \text{ when } t \le 0 \\ u = \exp(i\omega t),\ \theta = 1,\ \phi = 1, \text{ at } y = 0 \text{ when } t > 0 \\ u \to 0,\ \theta \to 0,\ \phi \to 0, \text{ for } y \to \infty \text{ when } t > 0 \end{array}\right\}. \tag{11}$$

3. Method of Solution

To get an exact closed form of solutions, we prefer to use a set of transformations. For purely an oscillating flow, the form of solutions for expressions (8), (9) and (10) can be considered as:

$$u(y, t) = u_0(y)\exp(i\omega t), \quad \theta(y, t) = \theta_0(y)\exp(i\omega t),$$

$$\phi(y, t) = \phi_0(y)\exp(i\omega t). \tag{12}$$

On using the forms of (12), expressions (8), (9), (10) and (11) give

$$\frac{d^2u_0}{dy^2} + \frac{du_0}{dy} - i\omega u_0 = -Gr\theta_0 - Gm\phi_0, \tag{13}$$

$$\frac{d^2\theta_0}{dy^2} + Pr\frac{d\theta_0}{dy} + (S - R - i\omega)Pr\theta_0 = 0, \tag{14}$$

$$\frac{d^2\phi_0}{dy^2} + Sc\frac{d\phi_0}{dy} - i\omega Sc\phi_0 = -SrSc\frac{d^2\theta_0}{dy^2}. \tag{15}$$

With initio-boundary conditions as:

$$\left.\begin{aligned} &u_0 = 1,\ \theta_0 = 1,\ \phi_0 = 1, \text{ at } y = 0 \text{ when } t > 0 \\ &u_0 \to 0,\ \theta_0 \to 0,\ \phi_0 \to 0, \text{ for } y \to \infty, \text{ when } t > 0 \end{aligned}\right\}. \tag{16}$$

The real part of expressions for non-dimensional temperature, concentration and velocity of fluid particles in the boundary layer are obtained as:

$$\theta_R(y, t) = \exp(-\alpha_1 y)\cos(\omega t - \beta_1 y), \tag{17}$$

$$\phi_R(y, t) = \gamma_5(y, t)\exp(-\alpha_1 y) + \gamma_6(y, t)\exp(-\alpha_2 y), \tag{18}$$

$$u_R(y, t) = \gamma_{17}(y, t)\exp(-\alpha_1 y) + \gamma_{18}(y, t)\exp(-\alpha_2 y) + \gamma_{19}(y, t)\exp(-\alpha_3 y). \tag{19}$$

Skin-friction at the plate:

The real part of the non-dimensional skin-friction coefficient at the plate is obtained as:

$$\tau_R = \left(\frac{\partial u_R}{\partial y}\right)_{y=0} = \tau_a \cos(\omega t) + \tau_b \sin(\omega t), \tag{20}$$

where

$$\tau_a = 2\tau_2 - \alpha_1(\tau_3 + y_3) - \alpha_2\tau_4 - \alpha_3(1 - \tau_3 - \tau_4 - y_3) + \beta_3(\tau_4 + \tau_6 + y_4),$$

$$\tau_b = \alpha_1(\tau_4 + y_4) + \alpha_2\tau_6 - \alpha_3(\tau_4 + \tau_6 + y_4) + \beta_1 x_5 + \beta_3(1 - \tau_3 - \tau_4 - y_3).$$

Rate of heat transfer coefficient:

The real part of the rate of heat transfer coefficient in terms of the Nusselt number is given as

$$Nu_R = -\frac{1}{Pr}\left(\frac{\partial \theta_R}{\partial y}\right)_{y=0} = \frac{1}{Pr}(\alpha_1 \cos(\omega t) - \beta_1 \sin(\omega t)). \tag{21}$$

Rate of mass transfer coefficient:

The real part of the rate of mass transfer coefficient in terms of the Sherwood number is

$$Sh_R = -\frac{1}{Sc}\left(\frac{\partial \phi_R}{\partial y}\right)_{y=0} = \frac{1}{Sc}(Sh_a \cos(\omega t) + Sh_b \sin(\omega t)), \tag{22}$$

where

$$Sh_a = \alpha_1 Sh_1 + \alpha_2(1 + Sh_1) + Sh_3 + Sh_5,$$

$$Sh_b = \alpha_1 Sh_2 + \alpha_2 Sh_2 + Sh_4 + Sh_6.$$

4. Results and Discussion

In order to get physical insight into the problem, the discussion in terms of graphs and tables for the velocity, temperature and concentration fields, viscous drag, rate of heat and mass transfers have been made by assigning

arbitrary numerical values to the parameters *Gr*, *Gm*, *Sr*, *Sc*, *S*, *R*, ω, *y* and *t*. In the study, air is considered to be a primary fluid (solvent), whose Prandtl number (*Pr*) is taken as 0.71 at 25°C or 298K and 1 atmosphere of pressure and to produce a significant effect on mass diffusion, some fluids considered as secondary (solute) such as Hydrogen, Water vapour, Oxygen, Ammonia and Carbon dioxide are diffused through air. The Schmidt numbers (*Sc*) of the corresponding secondary species are taken as, respectively, 0.22, 0.60, 0.74, 0.78, 0.98 and the Prandtl number of the diffused fluids is all considered as 0.71.

Figures 1 to 3 demonstrate the effect of the physical parameters such as Prandtl number (*Pr*), heat source parameter (*S*) and thermal radiation parameter (*R*) on the non-dimensional real part of temperature θ_R. Due to increase in values of *Pr* as well as *R*, the thickness of the thermal boundary layer diminishes, which results in decrease of the temperature variable near the plate. While a reverse effect is seen due to increase in values of *S* on θ_R. It is found that as *S* increases, θ_R also increases. The influence of Schmidt number (*Sc*) and Soret number (*Sr*) on the non-dimensional real part of concentration ϕ_R is shown graphically in Figures 4 and 5. It is clearly seen that as *Sc* increases, mass diffusivity D_M decreases near the plate surface, which results in the decrease of the thickness of concentration boundary layer thereby reducing the species concentration ϕ_R. On the other hand, as the values of *Sr* increases, the thickness of the concentration boundary layer rises, this increases the value of ϕ_R.

Figures 6, 7 and 8 depict how the rate of flow has been affected by the presence of the pertinent parameters like Prandtl number (*Pr*), Schmidt number (*Sc*) and thermal radiation parameter (*R*). It is observed that as *Pr* and *Sc* increase, the momentum diffusivity of the fluid particles increases near the plate, which results in increasing the velocity boundary layer thickness thereby decreasing the value of *u* and thus retard the motion. Whereas due to rise in values of *R*, the temperature near the plate decreases, which results in diminishing the thermal buoyancy force as a result the fluid

velocity u also decreases. The schematic representation of the effects of thermal buoyancy parameter (Gr), mass buoyancy parameter (Gm) and Soret number (Sr) on the fluid velocity u have been demonstrated in Figures 9 to 11. The increase in the parametric values of Gr as well as Gm is found to increase the thermal and mass buoyancy forces, respectively. Thus, the flow rate has found increasing due to increase in values of Gr and Gm. Again, due to increase in values of Sr, mass buoyancy force increases, this results an increase in values of u.

The influence of the thermal radiation parameter (R) on the viscous drag τ_R, Nusselt number Nu_R and Sherwood number Sh_R against time t has been shown graphically in Figures 12 to 14. The profile of viscous drag as well as Sherwood number is found in decreasing trend due to increase in values of R and t. On the other hand, a periodic change in values of Nu_R has been observed due to changes in values of R. It is also observed that for $t \in [0, 2.5]$, the heat transfer rate quantified by Nusselt number Nu_R increases due to increase in values of R, whereas it is found declining sharply as time progresses. When $t \in (2.5, 7]$, the value of Nu_R is seen dropping gradually, indicating the fall in heat transfer rate and thereafter for $t \in (7, 9]$, the value of Nu_R gradually increases, signifying the gained in momentum of the heat transfer rate. Figure 15 depicts the physical effect of heat source parameter S on the Nusselt number Nu_R against time t. When $t \in [0, 2.5]$, the value of Nu_R is seen decreasing as S increases, showing the declining trend of heat transfer rate and after that for $t > 2.5$, the heat transfer rate is found accelerating gradually till $t \approx 7$. Thereafter for $t > 7$, it is seen declining again as S increases.

The parametric effect of Soret number Sr on the skin-friction τ_R as well Sherwood number Sh_R against time t is expressed numerically in Tables 1 and 2, respectively. It is clearly seen that as the values of Sr and t increase, the frictional effect increases sharply, while a reverse effect has been observed on the values of Sh_R due to increase in values of Sr and t. It is

observed that for $Sr \in [1, 5]$, the values of Sh_R become negative, thus indicating the flow of mass from the fluid region to the plate surface.

5. Conclusion

A theoretical investigation has been done to study the physical effects of Soret, thermal radiation and heat generation parameter on the laminar homogeneous two-dimensional incompressible flow of a Newtonian constant viscous fluid under isothermal oscillating plate condition. Investigation reveals the following consequences:

- The fluid temperature decreases with increase in values of Prandtl number and thermal radiation parameter, whereas reversed effect is observed with increasing heat generation parameter.
- The concentration of the fluid particles reduces due to rise in values of Schmidt number, but is found increasing with increase in values of Soret number.
- The increase in values of the pertinent parameters like Schmidt number, Prandtl number and thermal radiation reduces the flow rate. While the velocity of the flow is found increasing as Soret number, thermal and solutal Grashof numbers increase.
- The effect of skin-friction on the plate is increased by the presence of Soret number whereas reverse effect has been observed under the presence of thermal radiation parameter against time.
- The increase in values of thermal radiation parameter alternately increases as well as decreases the Nusselt number, while an alternately decreasing as well as increasing trend of Nusselt number is observed due to an increase in values of heat source parameter against time.
- The Sherwood number is found decreasing in presence of Soret number and thermal radiation parameter against time.

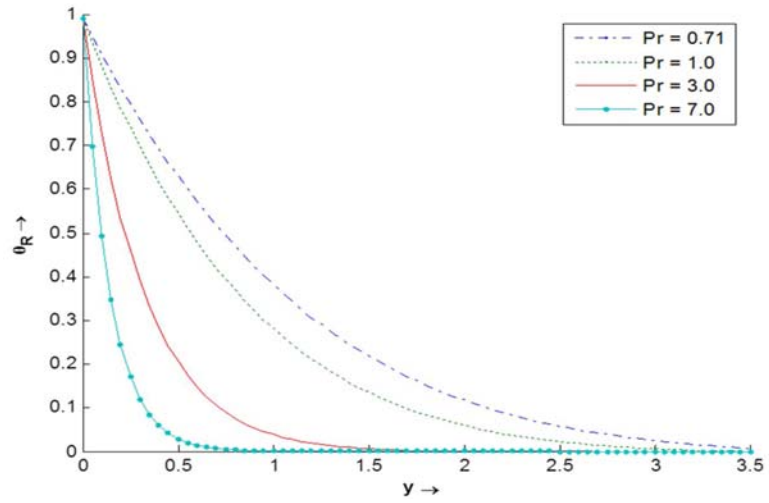

Figure 1. Temperature versus normal distance y for fixed values of $R = 0.5$, $t = 0.2$, $\omega = 0.7$, $S = 0.5$.

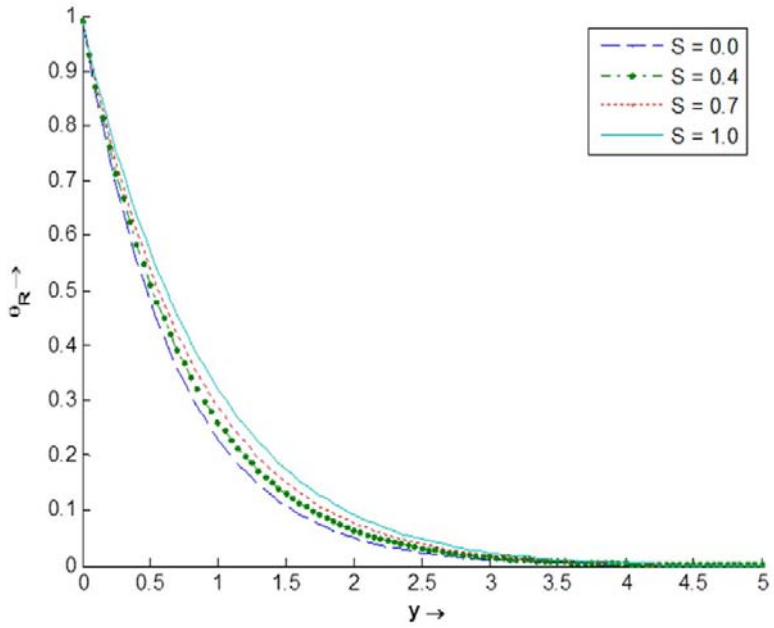

Figure 2. Temperature versus normal distance y for fixed values of $R = 0.5$, $t = 0.2$, $\omega = 0.7$, $S = 0.5$.

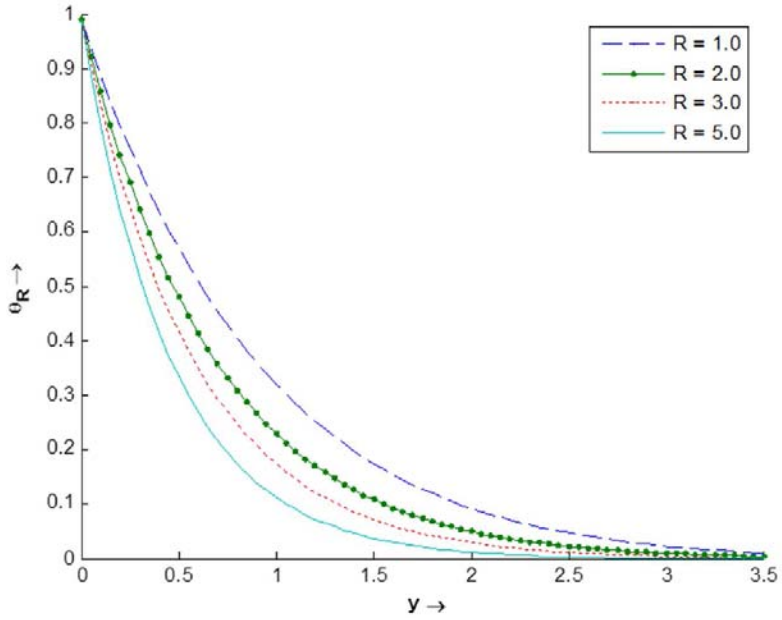

Figure 3. Temperature versus normal distance y for fixed values of $Pr = 0.71$, $t = 0.2$, $\omega = 0.7$, $S = 0.5$.

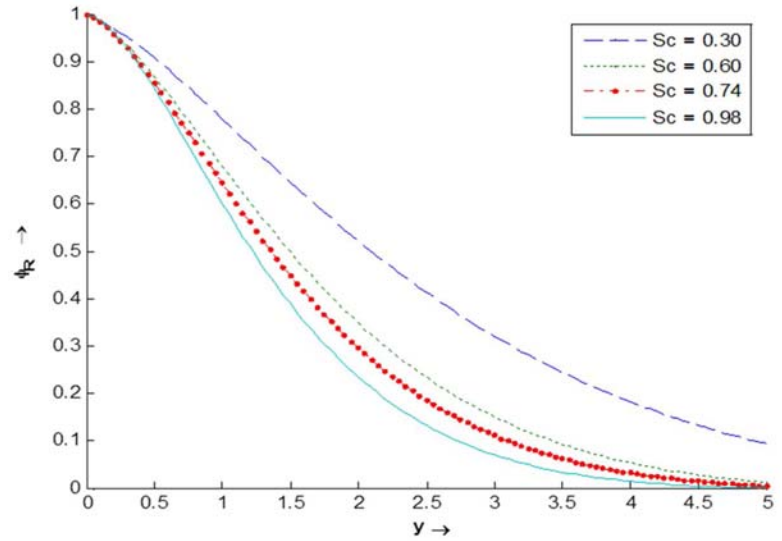

Figure 4. Concentration versus normal distance y for fixed values of $Pr = 0.71$, $t = 0.1$, $\omega = 0.3$, $Sr = 0.7$, $S = 0.2$, $R = 1.5$.

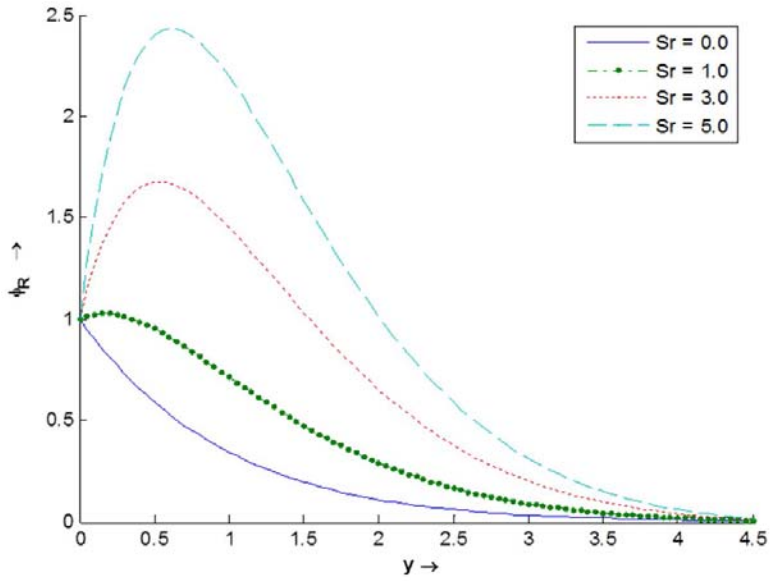

Figure 5. Concentration versus normal distance y for fixed values of Pr = 0.71, t = 0.1, ω = 0.3, Sc = 0.98, S = 0.2, R = 1.5.

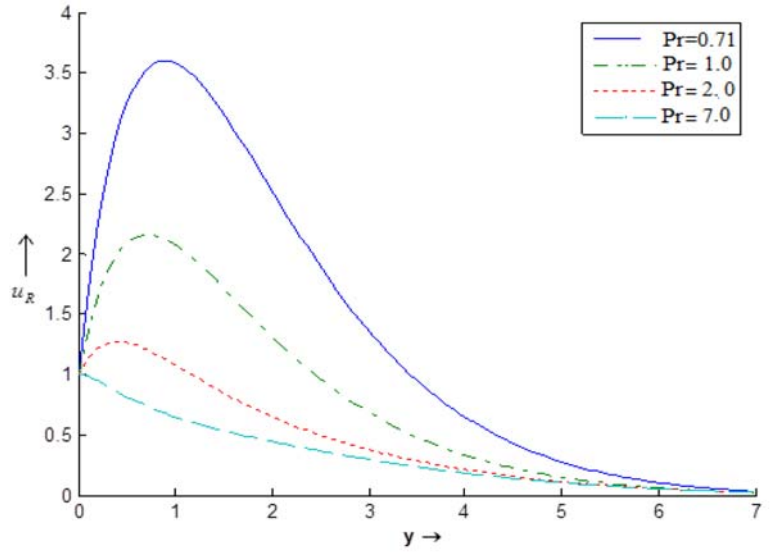

Figure 6. Velocity versus normal distance y for fixed values of Sr = 0.2, t = 0.1, ω = 0.2, Sc = 0.98, S = 0.1, R = 1.0, Gr = 6.0, Gm = 1.0.

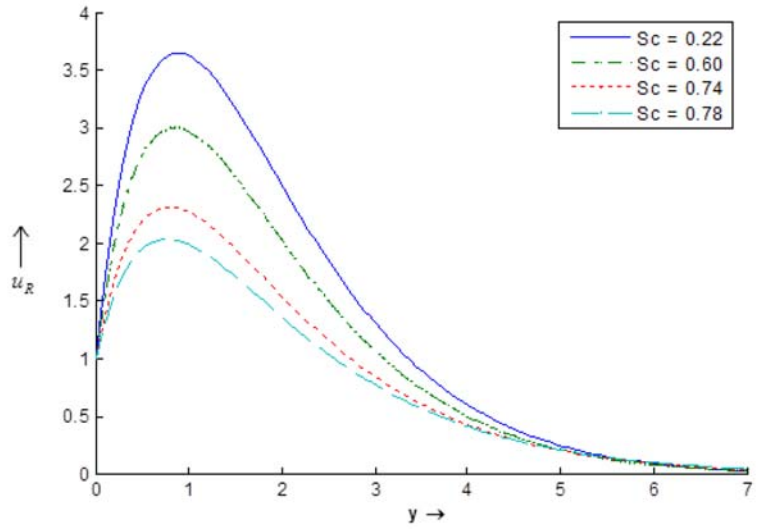

Figure 7. Velocity versus normal distance y for fixed values of $Sr = 0.2$, $t = 0.1$, $\omega = 0.2$, $Pr = 0.71$, $S = 0.1$, $R = 1.0$, $Gr = 6.0$, $Gm = 1.0$.

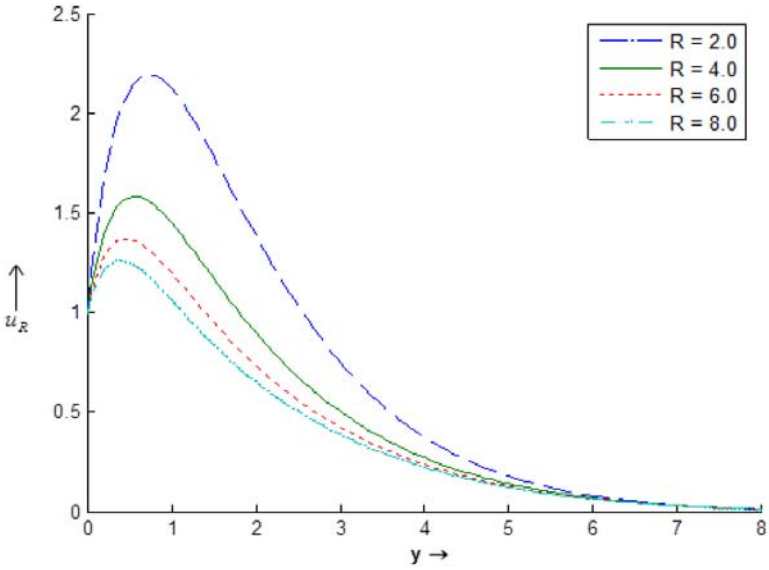

Figure 8. Velocity versus normal distance y for fixed values of $Sr = 0.2$, $t = 0.1$, $\omega = 0.2$, $Pr = 0.71$, $S = 0.1$, $Sc = 0.98$, $Gr = 6.0$, $Gm = 1.0$.

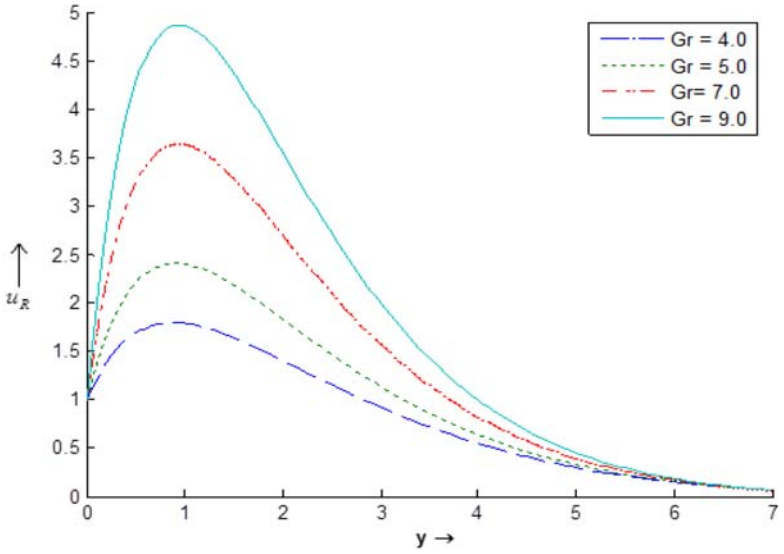

Figure 9. Velocity versus normal distance y for fixed values of $Sr = 0.2$, $t = 0.1$, $\omega = 0.2$, $Pr = 0.71$, $S = 0.1$, $Sc = 0.98$, $R = 1.0$, $Gm = 1.0$.

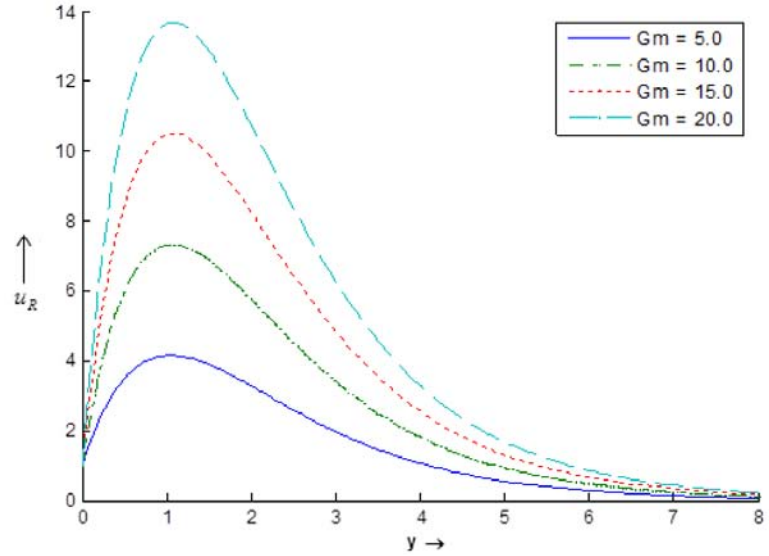

Figure 10. Velocity versus normal distance y for fixed values of $Sr = 0.2$, $t = 0.1$, $\omega = 0.2$, $Pr = 0.71$, $S = 0.1$, $Sc = 0.98$, $R = 1.0$, $Gm = 2.0$.

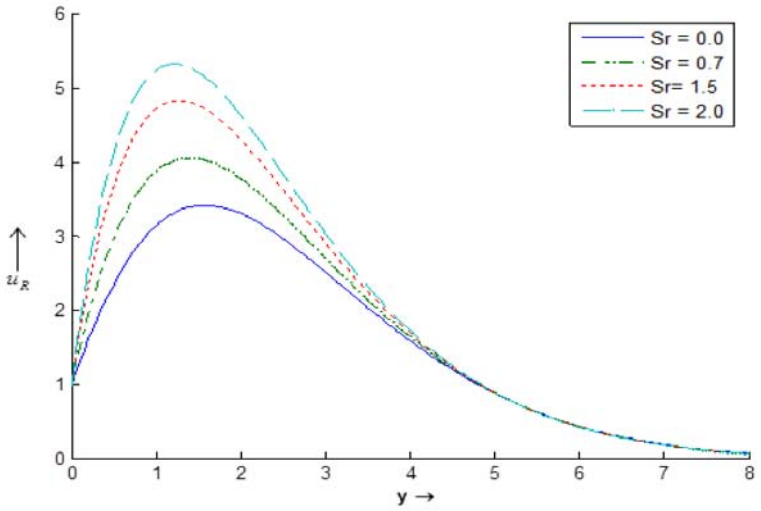

Figure 11. Velocity versus normal distance y for fixed values of $Gr = 10.0$, $Gm = 1.0$, $t = 0.1$, $\omega = 0.2$, $Pr = 0.71$, $S = 0.1$, $Sc = 0.98$, $R = 1.0$.

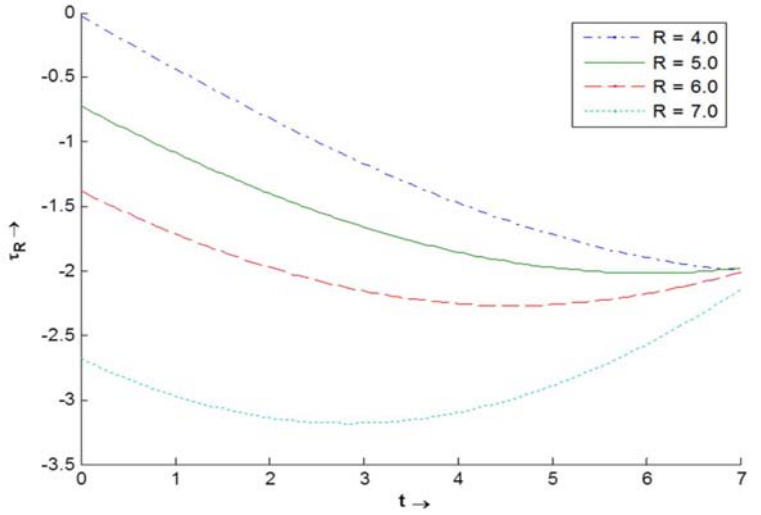

Figure 12. Skin-friction versus time t for fixed values of $Gr = 6.0$, $Gm = 1.0$, $\omega = 0.2$, $Pr = 0.71$, $S = 0.2$, $Sc = 0.98$, $Sr = 0.5$.

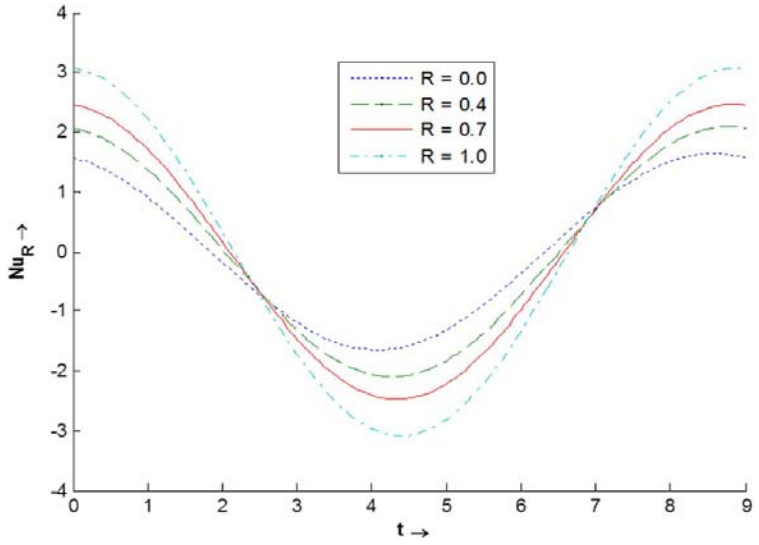

Figure 13. Nusselt number versus time t for fixed values of $\omega = 0.2$, $Pr = 0.71$, $S = 0.2$.

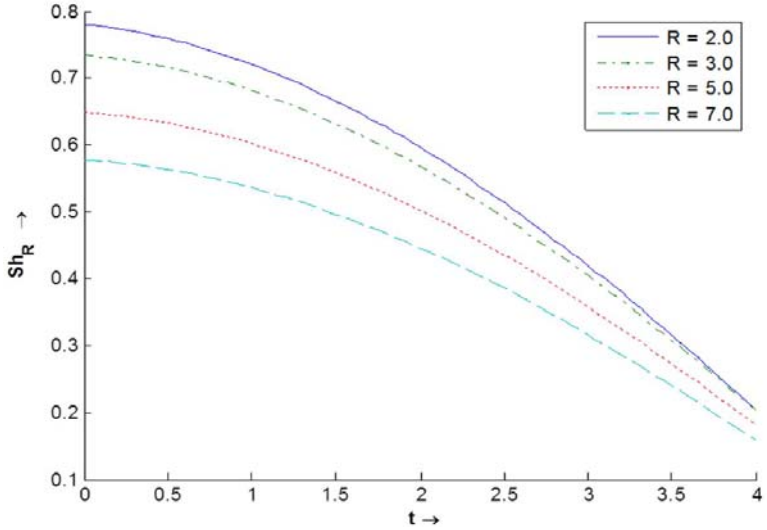

Figure 14. Sherwood number versus time t for fixed values of $Pr = 0.71$, $\omega = 0.2$, $S = 0.2$, $Sc = 0.98$, $Sr = 0.5$.

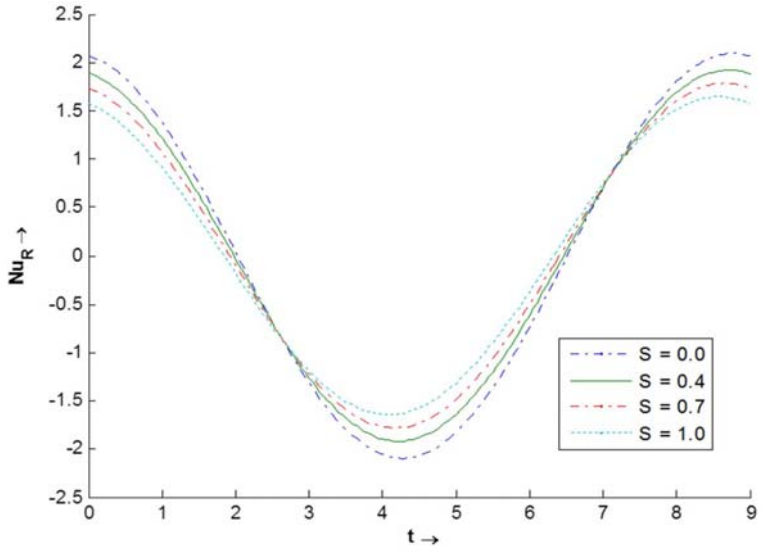

Figure 15. Nusselt number versus time t for fixed values of $Pr = 0.71$, $\omega = 0.2$, $R = 1.5$.

Table 1. Numerical values of skin-friction for different values of Soret number (Sr) against arbitrary values of t and for fixed values of $Pr = 0.71$, $Sc = 0.98$, $Gr = 10.0$, $Gm = 1.0$, $S = 1.0$, $R = 1.0$, $\omega = 0.2$

t	$Sr = 0.0$	$Sr = 0.7$	$Sr = 1.5$	$Sr = 2.0$
0.0	-3.7499	3.0627	10.8485	15.7147
0.5	-3.0741	4.8134	13.8277	19.4616
1.0	-2.3675	6.5160	16.6686	23.0140
1.5	-1.6373	8.1535	19.3430	26.3364
2.0	-0.8908	9.7095	21.8241	29.3958
2.5	-0.1353	11.1685	24.0872	32.1614
3.0	0.6215	12.5160	26.1092	34.6056
3.5	1.3721	13.7383	27.8711	36.7041
4.0	2.1090	14.8234	29.3542	38.4359
4.5	2.8249	15.7604	30.5439	39.7836
5.0	3.5125	16.5399	31.4285	40.7338

Table 2. Numerical values of Sherwood number for different values of Soret number (Sr) against arbitrary values of t and for fixed values of $Pr = 0.71$, $Sc = 0.98$, $S = 0.2$, $R = 1.5$, $\omega = 0.3$

t	$Sr = 0.0$	$Sr = 1.0$	$Sr = 3.0$	$Sr = 5.0$
0.0	1.0680	-0.3337	-3.1371	-5.9406
0.5	1.0560	-0.3991	-3.3092	-6.2193
1.0	1.0203	-0.4554	-3.4069	-6.3583
1.5	0.9617	-0.5016	-3.4280	-6.3545
2.0	0.8815	-0.5364	-3.3733	-6.2081
2.5	0.7814	-0.5593	-3.2407	-5.9222
3.0	0.6639	-0.5696	-3.0364	-5.5033
3.5	0.5314	-0.5670	-2.7639	-4.9608
4.0	0.3870	-0.5518	-2.4293	-4.3069
4.5	0.2339	-0.5241	-2.0402	-3.5562
5.0	0.0755	-0.4847	-1.6052	-2.7258

Appendix

$$\alpha_1 = \frac{1}{2}\left[Pr + \frac{\sqrt{Pr}}{\sqrt{2}}\sqrt{(Pr - 4(S-R) + \sqrt{(Pr - 4(S-R))^2 + 16\omega^2})}\right],$$

$$\beta_1 = \frac{\sqrt{Pr}}{2\sqrt{2}}\sqrt{(\sqrt{(Pr - 4(S-R))^2 + 16\omega^2} - (Pr - 4(S-R)))},$$

$$x_1 = \alpha_1^2 - \beta_1^2 + Sc\alpha_1,\ x_2 = 2\alpha_1\beta_1 + Sc\beta_1 - \omega Sc,$$

$$y_1 = x_1(\alpha_1^2 - \beta_1^2) + 2\alpha_1\beta_1 x_2,\ y_2 = 2\alpha_1\beta_1 x_1 - x_2(\alpha_1^2 - \beta_1^2)$$

$$\gamma_1(y) = -\frac{SrSc}{x_1^2 + x_2^2}(y_1\cos(\beta_1 y) + y_2\sin(\beta_1 y)),$$

$$\gamma_2(y) = -\frac{SrSc}{x_1^2 + x_2^2}(y_2\cos(\beta_1 y) - y_1\sin(\beta_1 y)),$$

$$\alpha_2 = \frac{1}{2}\left[Sc + \frac{\sqrt{Sc}}{\sqrt{2}}\sqrt{(Sc + \sqrt{Sc^2 + 16\omega^2})}\right],$$

$$\beta_2 = \frac{\sqrt{Sc}}{2\sqrt{2}}\sqrt{(\sqrt{Sc^2 + 16\omega^2} - Sc)},$$

$$\gamma_3(y) = ((1 - \gamma_1(y))\cos(\beta_2 y) - \gamma_2(y)\sin(\beta_2 y)),$$

$$\gamma_4(y) = -((1 - \gamma_1(y))\sin(\beta_2 y) + \gamma_2(y)\cos(\beta_2 y)),$$

$$\gamma_5(y, t) = \gamma_1(y)\cos(\omega t) - \gamma_2(y)\sin(\omega t),$$

$$\gamma_6(y, t) = \gamma_3(y)\cos(\omega t) - \gamma_4(y)\sin(\omega t),$$

$$\gamma_7(y, t) = \gamma_2(y)\cos(\omega t) + \gamma_1(y)\sin(\omega t),$$

$$\gamma_8(y, t) = \gamma_4(y)\cos(\omega t) + \gamma_3(y)\sin(\omega t),$$

$$\alpha_3 = \frac{1}{2}\left[1 + \frac{1}{\sqrt{2}}\sqrt{(1 + \sqrt{1 + 16\omega^2})}\right],\ \beta_3 = \frac{1}{2\sqrt{2}}\sqrt{(\sqrt{1 + 16\omega^2} - 1)},$$

$$x_3 = \alpha_1^2 - \beta_1^2 - \alpha_1,\ x_4 = 2\alpha_1\beta_1 - \beta_1 - \omega,$$

$$y_3 = -\frac{x_3 Gr}{x_3^2 + x_4^2},\ y_4 = \frac{x_4 Gr}{x_3^2 + x_4^2},$$

$$\gamma_9(y) = -\frac{Gm((\alpha_1^2 - \alpha_1)\gamma_1(y) - \omega\gamma_2(y))}{(\alpha_1^2 - \alpha_1)^2 + \omega^2},$$

$$\gamma_{10}(y) = -\frac{Gm((\alpha_1^2 - \alpha_1)\gamma_2(y) + \omega\gamma_1(y))}{(\alpha_1^2 - \alpha_1)^2 + \omega^2},$$

$$\gamma_{11}(y) = -\frac{Gm((\alpha_2^2 - \alpha_2)\gamma_3(y) - \omega\gamma_4(y))}{(\alpha_2^2 - \alpha_2)^2 + \omega^2},$$

$$\gamma_{12}(y) = -\frac{Gm((\alpha_2^2 - \alpha_2)\gamma_4(y) + \omega\gamma_3(y))}{(\alpha_2^2 - \alpha_2)^2 + \omega^2},$$

$$\gamma_{13}(y) = \gamma_{11}(y) + \gamma_9(y)\cos(\beta_1 y) + \gamma_{10}(y)\sin(\beta_1 y),$$

$$\gamma_{14}(y) = \gamma_{12}(y) + \gamma_{10}(y)\cos(\beta_1 y) - \gamma_9(y)\sin(\beta_1 y),$$

$$\gamma_{15}(y) = (1 - \gamma_{10}(y) - \gamma_{13}(y))\cos(\beta_3 y) - (\gamma_{11}(y) + \gamma_{14}(y))\sin(\beta_1 y),$$

$$\gamma_{16}(y) = -((\gamma_{11}(y) + \gamma_{14}(y))\cos(\beta_3 y) + (1 - \gamma_{10}(y) - \gamma_{13}(y))\sin(\beta_1 y)),$$

$$\gamma_{17}(y, t) = \gamma_{13}\cos(\omega t) - \gamma_{14}\sin(\omega t),$$

$$\gamma_{18}(y, t) = \gamma_{10}(y)\cos(\omega t) - \gamma_{11}(y)\sin(\omega t),$$

$$\gamma_{19}(y, t) = \gamma_{15}(y)\cos(\omega t) - \gamma_{16}(y)\sin(\omega t).$$

Acknowledgement

The first author (SSG) thankful to UGC, New Delhi, India for providing the financial support to conduct this research work under UGC MRP no. 41-1382/2012(SR).

References

[1] N. Ahmed and S. Sengupta, Thermo-diffusion and diffusion-thermo effects on a three dimensional MHD mixed convection flow past an infinite vertical porous plate with thermal radiation, J. of Magneto Hydrodynamics 47 (2011), 41-60.

[2] N. Ahmed, S. Sengupta and D. Datta, An exact analysis for MHD free convection mass transfer flow past an oscillating plate embedded in a porous medium with soret effect, Chem. Eng. Comm. 200 (2013), 494-513.

[3] O. Aydin and A. Kaya, Radiation effect on MHD mixed convection flow about a permeable vertical plate, Heat Mass Transfer 45 (2008), 239-246.

[4] R. D. Cess, The interaction of thermal radiation with free convection heat transfer, Int. J. Heat Mass Trans. 9 (1966), 269-277.

[5] A. J. Chamkha, Unsteady MHD convective heat and mass transfer past a semi-infinite vertical permeable moving plate with heat absorption, Internat. J. Engrg. Sci. 24 (2004), 217-230.

[6] A. C. Cogly, W. C. Vincentine and S. E. Gilles, Differential approximation for radiative transfer in a non-gray gas near equilibrium, AIAA Journal 6 (1968), 551-555.

[7] U. N. Das, A small unsteady perturbation on the steady hydromagnetic boundary layer flow past a semi-infinite plate, Proc. Camb. Phil. Soc. 68 (1970), 509-528.

[8] C. D. S. Devi and M. Nagaraj, Heat and mass transfer in unsteady magneto hydrodynamic flow over a semi-infinite flat plate, Indian J. Pure Appl. Math. 15 (1984), 1148-1161.

[9] Z. Dursunkaya and W. M. Worek, Diffusion-thermo and thermo-diffusion effects in transient and steady natural convection from vertical surface, Int. J. Heat Mass Trans. 35 (1992), 2060-2065.

[10] E. R. G. Eckert and R. M. Drake, Analysis of Heat and Mass Transfer, Hemisphere Pub. Corp., Washington, D.C, 1972.

[11] M .Y. Gokhale and F. M. AL Samman, Effects of mass transfer on the transient free convection flow of a dissipative fluid along a semi-infinite vertical plate with constant heat flux, Int. J. Heat Mass Trans. 46 (2003), 999-1011.

[12] R. Gulab and R. Mishra, Unsteady flow through magnetodydrodynamic porous media, Indian J. Pure Appl. Math. 8 (1977), 637-642.

[13] M. A. Hossain and H. S. Takhar, Radiation effect on mixed convection along a vertical plate with uniform surface temperature, Heat Mass Transfer 31 (1996), 243-248.

[14] D. T. J. Hurle and E. Jakeman, Soret-driven thermo-solutal convection, J. Fluid Mech. 47 (1971), 667-687.

[15] N. C. Jain and P. Gupta, Unsteady hydromagnetic thermal boundary layer flow past an infinite porous surface in the slip flow regime, Ganita 56 (2005), 15-25.

[16] A. A. Megahed, Unsteady MHD flow through porous medium bounded by a porous plate, Indian J. Pure Appl. Math. 15 (1984), 1140-1147.

[17] A. Postelnicu, Influence of a magnetic field on heat and mass transfer by natural convection from vertical surfaces in porous medium considering Soret and Dufour effects, Int. J. Heat Mass Trans. 47 (2004), 1467-1472.

[18] L. Rayleigh, On the motion of solid bodies through viscous liquid, Phil. Mag. 21 (1911), 697-711.

[19] Sanjib Sengupta, Thermal diffusion effect of free convection mass transfer flow past a uniformly accelerated porous plate with heat sink, International Journal of Mathematical Archive 2 (2011), 1266-1273.

[20] Sanjib Sengupta, Radiative mixed convection mass transfer flow past an iso-thermal porous plate embedded in a permeable medium in presence of thermal diffusion and heat generation, International Journal of Computer Applications 40 (2012), 17-22.

[21] V. M. Soundalgekar, Free convection effects on the flow past a vertical oscillating plate, Astrophysics and Space Science 64 (1979), 165-172.

[22] G. G. Stokes, On the effect of the internal friction of fluids on the motion of pendulums, Trans. Camb. Phil. Soc. IX (1851).